RADIO-FREQUENCY SIZE EFFECT IN A MAGNETIC FIELD PERPENDICULAR TO THE SURFACE OF A METAL

V. F. GANTMAKHER and É. A. KANER

Institute of Solid State Physics, Academy of Sciences U.S.S.R.; Institute of Radio
Engineering and Electronics, Academy of Sciences, Ukrainian S.S.R.

We investigate experimentally and theoretically a new radio-frequency size effect in metal samples placed in a magnetic field perpendicular to their surface. The effect is due to the "ineffective" electrons moving along a helical path inside the metal. Because of this motion, a slowly damped field component is produced in the volume of the metal, and leads to oscillations of the impedance of a plane-parallel plate. The oscillations are periodic in a straight field. The periods ΔH are determined by the extremal values of the electron displacements along the magnetic field within one cyclotron period. Two types of electron trajectories that can lead to such oscillations are considered. The experiments were carried out with single-crystal tin in a magnetic field nearly parallel to the [100] crystallographic axis.

1. INTRODUCTION

ALL the known radio-frequency size effects in metallic single crystals at low temperatures are due to different groups of so-called effective electrons, which move on individual sections of their trajectories parallel to the surface of the metal. These size effects constitute a manifestation of the system of peaks of alternating fields and currents existing in the volume of the metal, the depth variation of the distance between which is determined by the characteristic dimensions of the electron trajectories in the magnetic field **H**. The sequence of peaks can be due to chains of trajectories of electrons having identical momentum projections along **H** but situated at different depths[1-3]. The peaks can also be connected with electrons that move along a periodic trajectory from the surface inside the metal[4,5].

We have investigated experimentally and theoretically size effects of another type, due to the motion of ineffective electrons inside the metal. The trajectories of these electrons are such that their normal velocity v_z never vanishes (the z axis is directed along the normal **n** to the surface of the metal). The interaction between the electron and the electromagnetic field is therefore approximately the same along the entire trajectory. The average interaction energy differs from zero only for that harmonic of the alternating field in metal, whose wavelength λ is equal to the displacement of the electron u in one cyclotron period. In the case of the effective electrons, on the other hand, the interaction differs from zero also for multiple harmonics $\lambda_n = u/n$ (n = 1, 2, 3, ...). This difference causes the sharp peaks of field within the volume of the metal (and the narrow lines of the size effect) to give way in the case of the ineffective electrons to a harmonic distribution of the field inside the metal. As usual, the spatial period of the oscillations should be determined by the extremal values $u = u_{ext}$.

The extremum of u as a function of the quasi-momentum component p_H along the field must be reached at the elliptic limiting point:

$$u_0 = 2\pi c / eHK^{1/2} \qquad (1)$$

(K —value of the Gaussian curvature of the Fermi surface at the limiting point). In the case of a non-ellipsoidal Fermi surface, other extrema of the function $u(p_H)$ are also possible:

$$u_1 = \frac{c}{eH}\left|\frac{\partial S}{\partial p_H}\right|_{ext}, \qquad (2)$$

where $S(p_H)$ is the area of intersection of the Fermi surface with the plane $p_H = $ const. The expansion of $u(p_H) - u_0$ in powers of $p_H - p_{H\,max}$ begins with the linear term, while the expansion of $u(p_H) - u_1$ in powers of $p_H - p_{H_1}$ begins with the quadratic term. The difference between cases (1) and (2) is due to the fact that near the limiting point the electrons move on spirals of very small radius; on

the other hand, the radius of the spiral trajectories of the electrons near other sections with extremal value of $u(p_H)$ is far from small.

This effect, unlike the other radio-frequency size effects, has an analog in static conductivity. It is shown in the theoretical paper of Sondheimer[6], and later by V. Gurevich[7], that the static conductivity of metallic plates has a term that oscillates with the field and is connected with the number of electron revolutions on the path from one surface of the plate to the other. This effect was first observed by Babiskin and Siebenmann[8] and by others[9,10].

2. THEORY

In this section we find the distribution of the electromagnetic field in a half-space $z > 0$ occupied by a metal, with $\mathbf{H} \parallel Oz$. For simplicity we assume that the Fermi surface is singly-connected and is axially-symmetrical with respect to the Oz axis. As is well known[11,12], the distribution of the circularly polarized components of the electromagnetic field in a metal has the following form:

$$E_\pm(z) \equiv E_x(z) \pm iE_y(z)$$

$$= -\frac{1}{\pi} E_\pm'(0) \int_0^\infty \frac{dk(e^{ikz} + e^{-ikz})}{k^2 - 4i\pi\omega c^{-2}\sigma_\pm(k)}. \tag{3}$$

Here $E_\alpha(z)$ —intensity of the alternating electric field

$$(\mathbf{E}(z,t) = \mathbf{E}(z)e^{-i\omega t}), \quad E_\pm'(0) \equiv \partial E_\pm(0) / \partial z,$$

ω and k are the frequency and wave vector of the electromagnetic wave, and for circularly polarized waves the Fourier components $\sigma_\pm(k)$ of the conductivity are

$$\sigma_\pm(k)$$

$$= \int_{-p_{z\,max}}^{p_{z\,max}} \frac{2\pi e^2}{(2\pi\hbar)^3} dp_z \frac{m}{\Omega} v_\perp^2 \left[\gamma \mp i + i\frac{ku(p_z)}{2\pi}\right]^{-1}, \tag{4}$$

where e and m are the absolute values of the charge and of the effective mass of the electron, $\Omega = eH/mc$ the cyclotron frequency, $\gamma = \nu/\Omega$, γ the frequency of collision between the electrons and the scatterers, $v_\perp(p_z) = (v_x^2 + v_y^2)^{1/2}$, and the displacement in one period is $u = 2\pi v_z/\Omega$. The $\pm$ signs in (4) correspond to electrons; in the case of holes they should be reversed. Expression (4) can be readily obtained from the kinetic equation (see [12]).

For a spherical Fermi surface we obtain from (4)

$$\sigma_\pm(k) = \pm \frac{3i}{2} \frac{Ne^2}{kp} \left[a_\pm - \frac{(1 - a_\pm^2)}{2} \ln \frac{a_\pm - 1}{a_\pm + 1}\right], \tag{5}$$

$$a_\pm = (\Omega \pm i\nu) / kv, \quad N = p^3 / 3\pi^2\hbar^3. \tag{6}$$

Formula (3) is exact when the electrons are specularly reflected from the interface. In the case of diffuse reflection, on the other hand, it describes correctly the field distribution apart from a numerical factor of order unity (see also [11,1]).

As is known from the paper of Reuter and Sondheimer[11], in the case of the anomalous skin effect the expression for the field in the metal contains two terms. One is the contribution from the poles of the integrand in (3) and describes the sharp decrease in the field near the metal surface. The other term is due to the presence of isolated branch points of the integrand and yields a small but rather slowly damped (over distances on the order of the mean free path l of the electrons) field component. The isolated branch points of the Fourier component of the conductivity $\sigma_\pm(k)$ are due to the contribution made by the electrons near the sections with $u(p_z) = u_{ext}$. In a strong magnetic field, when $\gamma \ll 1$, these branch points are located near the real axis on the complex k plane.[1] At large distances from the surface of the metal, the contribution of the poles to the integral (3) can be neglected, and the behavior of the field will be determined by the behavior of the function $\sigma_\pm(k)$ near the branch points.

A. Case of limiting point. The contribution made to the conductivity by the electrons situated in the vicinity of the limiting point is determined by the integral

$$\Delta\sigma_\pm = \frac{e^2}{4\pi^2\hbar^3} \frac{m}{\Omega} \frac{\partial v_\perp^2}{\partial p_z} \Bigg\{ - \int^{p_{z\,max}} dp_z(p_{z\,max} - p_z)$$

$$\times \left[\gamma \mp i + i\frac{ku_0}{2\pi} - i\frac{ku_0'}{2\pi}(p_{z\,max} - p_z)\right]^{-1}$$

$$- \int_{-p_{z\,max}} dp_z(p_z + p_{z\,max})$$

$$\times \left[\gamma \mp i - i\frac{ku_0}{2\pi} + i\frac{ku_0'}{2\pi}(p_z + p_{z\,max})\right]^{-1}\Bigg\}$$

$$= i\frac{e^2}{\hbar^3} \frac{m}{\Omega} \frac{\partial v_\perp^2}{\partial p_z}\left(\frac{1}{ku_0'}\right)^2$$

---

[1]The anomalous penetration of the field connected with the drifting of the effective electrons[4] (field peaks) is due from the mathematical point of view to the presence of an infinite sequence of equidistant branch points of the function $\sigma(k)$ near the real axis. The case of the chain of orbits[1,3] is connected with the presence of a periodic sequence of zeros of the function $\sigma(k)$.

$$\times \left[\left(-i\gamma \mp 1 + \frac{ku_0}{2\pi} \right) \ln \left(-i\gamma \mp 1 + \frac{ku_0}{2\pi} \right) \right.$$

$$\left. + \left(-i\gamma \mp 1 - \frac{ku_0}{2\pi} \right) \ln \left(-i\gamma \mp 1 - \frac{ku_0}{2\pi} \right) \right]. \quad (7)$$

The integration is carried out here in the vicinity of the limiting points with $|p_z| = p_{z\,max}$ on the Fermi surface $\epsilon(p) = \epsilon_F$; the values of these quantities are taken at $\epsilon = \epsilon_F$, $p_z = p_{z\,max}$, and $u_0' = \partial u(p_{z\,max})/\partial p_z$.

We see from (7) that near the positive real axis the function $\sigma_+(k)$ has a logarithmic branch point at $k_+ = 2\pi(1+i\gamma)/u_0$, while the function $\sigma_-(k)$ has one at $k_- = 2\pi(1-i\gamma)/u_0$. Let us calculate, for example, the asymptotic behavior of the function $E_+(z)$ at very large z, due to the contribution made to (3) by the branch point k_+. We draw a cut in the complex k plane from the point k_+ parallel to the imaginary axis in the direction of Im $k > 0$. We bend the contour integral towards Im $k > 0$ in the term of (3) containing e^{ikz}, and towards Im $k < 0$ in the term with e^{-ikz}. Then the expression (3) for $E_+(z)$ can be represented as the sum of the residues and the integral along the edges of the cut (contour C, see Fig. 1):

$$-\pi \frac{E_+(z)}{E_+'(z)} = 2\pi i \sum \text{Res} + \int_C \frac{dk\, e^{ikz}}{k^2 - i4\pi\omega c^{-2}\sigma_+(k)}. \quad (8)$$

The sum of the integrals along the imaginary axis vanishes identically. The sum of the residues, as indicated above, is a rapidly decreasing function of z, inasmuch as the roots of the dispersion equation

$$k^2 - 4\pi i\omega c^{-2}\sigma_+(k) = 0$$

are essentially complex and are determined by the effective electrons: $k_\alpha = \delta_0^- \epsilon_\alpha$, where $\epsilon_\alpha^3 = i$ ($\alpha = 1, 2, 3$). The quantity δ_0 is the depth of penetration of the electromagnetic field into the metal when H = 0:

$$\delta_0^{-3} = \omega e^2 c^{-2} \hbar^{-3} \sum \int dp_z m v_\perp^2 \delta(v_z), \quad (9)$$

where $\delta(v_z)$ is the Dirac delta function; the summation is over all the bands.

Taking into account the non-uniqueness of the function $\sigma_+(k)$ on the different edges of the cut, we first evaluate the integral in (8) and then represent $E_+(z)$ in the form

$$\frac{E_+(z)}{E_+'(0)} = \frac{A_0}{z^2} \exp \left(ik_+z - i\frac{\pi}{2} \right), \quad (10)$$

$$A_0 = \frac{c^2}{\omega} \frac{e^2}{(2\pi\hbar)^3} \frac{m|v_z|}{\Omega} \left| \frac{\partial v_\perp^2}{\partial p_z} \right| \left(\frac{u_0}{u_0'} \right)^2 \sigma_+^{-2} \left(\frac{2\pi}{u_0} \right). \quad (11)$$
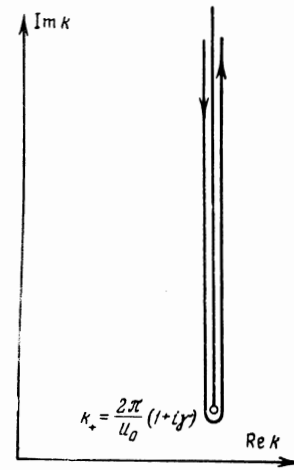
For a spherical Fermi surface, using (5), we

FIG. 1

obtain

$$A_0 = -\tfrac{1}{4}\pi\delta_0^3, \qquad \delta_0^3 = c^2 p / 3\pi^2\omega Ne^2. \quad (12)$$

To estimate the relative oscillation amplitude of (10) in the presence of two different limiting points, we can consider a model in which the Fermi surface consists of two spheres with radii p_1 and p_2. Using (5) and (11), we obtain

$$\frac{A_0^{(1)}}{A_0^{(2)}} = \frac{N_1 p_1}{N_2 p_2} \frac{\sigma_+^2(2\pi/u_0^{(2)})}{\sigma_+^2(2\pi/u_0^{(1)})}$$

$$= \xi^2 \left[\frac{2}{1-\xi} + \ln \frac{1-\xi}{1+\xi} \right]^2 \Big/ \left[\frac{2\xi}{1-\xi} - \ln \frac{1-\xi}{1+\xi} - i\pi \right]^2, \quad (13)$$

where $\xi = p_1/p_2 < 1$. When ξ is small the ratio of the amplitudes is $-4\pi^{-2}\xi^2$. We see from (11) and (13) that the oscillations due to different limiting points can have different phases, since σ_+^2 is complex.

It follows from (10) that at large distances from the metal surface

$$E_x(z) = \frac{|A_0|}{z^2} e^{-z/l}$$

$$\times \left[E_x'(0) \sin \left(\frac{2\pi z}{u_0} + \chi \right) + E_y'(0) \cos \left(\frac{2\pi z}{u_0} + \chi \right) \right],$$

$$E_y(z) = \frac{|A_0|}{z^2} e^{-z/l} \left[-E_x'(0) \cos \left(\frac{2\pi z}{u_0} + \chi \right) \right.$$

$$\left. + E_y'(0) \sin \left(\frac{2\pi z}{u_0} + \chi \right) \right], \quad (14)$$

where $\chi = \arg A_0$.

B. Case of extremal helical trajectory. In the vicinity of the corresponding branch point, the Fourier component of the conductivity $\sigma_\pm(k)$ is given by

$$\sigma_{\pm}(k) = \frac{e^2}{4\pi^2\hbar^3} \frac{mv_{\perp}^2}{\Omega} \Big\{ \int_{-\infty}^{\infty} dp_z$$

$$\times \left[\gamma \mp i + i\frac{ku_1}{2\pi} - i\frac{k|u_1''|}{4\pi}(p_z - p_{z1})^2 \right]^{-1}$$

$$+ \int_{-\infty}^{\infty} dp_z \left[\gamma \mp i - i\frac{ku_1}{2\pi} + i\frac{k|u_1''|}{4\pi}(p_z - p_{z1})^2 \right]^{-1} \Big\}$$

$$\cong \frac{e^2}{4\pi^2\hbar^3} \frac{mv_{\perp}^2}{\Omega} \left(\frac{2|u_1|}{|u_1''|} \right)^{1/2} \frac{e^{\pm i\pi/2}}{(1 \pm i\gamma - ku_1/2\pi)^{1/2}} . \quad (15)$$

All quantities are taken at the point $|p_z| = p_{zi}$, where $u(p_z)$ has an extremum, $u_1'' = (\partial^2 u/\partial p_z^2)_{p_{z1}}^s$.

Unlike in the case of the limiting point, here $\sigma_{\pm}(k)$ acquires branch points of second order when $k_{\pm} = 2\pi u_1^{-}(1 \pm i\gamma)$. Calculations analogous to those made above lead to the following formulas for the field:

$$E_x(z) = \frac{A_1}{u_1^{1/2} z^{3/2}} e^{-z/l_1}$$

$$\times \left[E_x'(0)\cos\left(\frac{2\pi z}{u_1} + \frac{\pi}{4}\right) - E_y'(0)\sin\left(\frac{2\pi z}{u_1} + \frac{\pi}{4}\right) \right],$$

$$E_y(z) = \frac{A_1}{u_1^{1/2} z^{3/2}} e^{-z/l_1} \left[E_x'(0)\sin\left(\frac{2\pi z}{u_1} + \frac{\pi}{4}\right) \right.$$

$$\left. - E_y'(0)\cos\left(\frac{2\pi z}{u_1} + \frac{\pi}{4}\right) \right]; \quad (16)$$

$$A_1 = \frac{c^2}{\omega} \frac{\hbar^3}{e^2} \frac{|v_z|}{mv_{\perp}^2} \left| \frac{u_1''}{u_1} \right|^{1/2} \sim \delta_0^3, \qquad l_1 = \frac{|v_{z1}|}{\nu}. \quad (17)$$

All the formulas given above are valid when the conditions $\delta_0 \ll u \ll l, z$ are satisfied.

Comparison of (14) and (16) shows that in the case of a helical trajectory the amplitude of the oscillations is $(z/u)^{1/2}$ times larger than in the case of a limiting point; the amplitude of the oscillations due to the electrons near the limiting point is independent of the magnetic field.

The obtained field distribution is quite peculiar. An electron penetrating into the metal carries information concerning the instantaneous value of the electric field **E** in the skin layer, the vector **E** following a helical path (we recall that $\omega \ll \nu$). When the external field is linearly polarized, a standing helical wave is produced. If the external field is circularly polarized, a wave is obtained with positive or negative phase velocity, depending on the relation between the rotation of the polarization vector of the external field to the direction of rotation of the electrons.

So far we have considered only the simplest case of an axially symmetrical Fermi surface, when the longitudinal component of the velocity v_z is independent of τ ($\tau = \Omega t$ is the dimension-

less time of motion of the electron along the orbit in momentum space), and the transverse components v_x and v_y contain only the first harmonics in τ:

$$v_x = v_{\perp}\cos\tau, \qquad v_y = v_{\perp}\sin\tau.$$

In the general case the fact that v_z is a function of τ and the presence of higher harmonics in the Fourier expansions of $v_x(\tau)$ and $v_y(\tau)$ leads to the occurrence of new branch points of the functions $\sigma_{\pm}(k)$ at $k = 2\pi u^{-1}(n \pm i\gamma)$ ($n = 2, 3, \ldots$). This in turn leads to the appearance of higher harmonics in $E(z)$. In particular, points with $v_z(\tau) = 0$ can appear on the extremal helical trajectory when the longitudinal velocity component v_z has a strong dependence on τ. The electrons become effective, and the interference of a large number of higher-order harmonics results in narrow field peaks. The strong dependence of v_z on τ should also lead to a dependence of the oscillation amplitude on the polarization of the external field. On the other hand, for an elliptical limiting point, the degree of ellipticity of the standing helical wave (14) coincides with the ellipticity of the limiting point itself.

3. EXPERIMENT

We employed in the experiments the previously used[13,4] modulation procedure for measuring the dependence of the imaginary part of the surface impedance of a metallic sample on the magnetic field. The sample was placed inside a tank-circuit coil, and the variation of the oscillation frequency f with the field was measured. The measured quantity was

$$\frac{\partial f}{\partial H} \sim -\frac{\partial}{\partial H}\delta_{\mathrm{eff}} = \frac{\partial}{\partial H}\left[\mathrm{Re}\,\frac{E(0) - E_d}{E'(0)} \right]$$

$$= -\frac{\partial}{\partial H}\left[\mathrm{Re}\,\frac{E_d}{E'(0)} \right], \quad (18)$$

where E_d is the electric field on the other side of the plate, due to the penetration of the wave into the metal. Inasmuch as the distribution of the field in a plate of thickness $d \gg u$ should not differ, for diffusely scattered electrons, from the distribution of the field in a half-space, the experimental curves can be directly compared with formulas (14) and (16) for $E_x(z, H)$ by putting $E_y'(0) = 0$ and $z = d$: $E_d(H) = E_x(d, H)$. (The field H enters in (14) and (16) as a parameter.)

The experiments were made with tin samples grown in dismountable quartz molds[14] from metal containing $\sim 10^{-4}\%$ impurities. The sam-
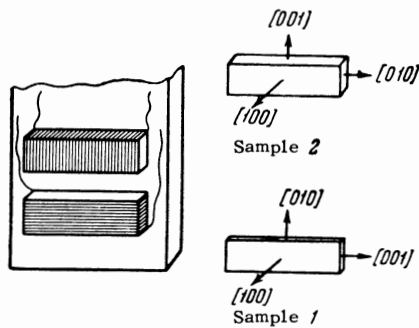
FIG. 2

ples were rectangular plates measuring 13×3 mm; we had to give up the previously employed larger-diameter discs because of the need for modulating the field perpendicular to the surface of the sample, the depth of penetration of the field at 20 cps being on the order of 1 mm under our conditions. The orientations of the two samples, with which we obtained all the main results, are shown in Fig. 2 (the angle between the normals to the surface and the [100] axis did not exceed 1.5°). Sample 1 had a thickness $d_1 = 0.46$ mm and sample 2 a thickness $d_2 = 0.96$ mm.

The sample occupied the greater part of the interior of the tank-circuit coil. The shape of the sample was such that it could not be rotated on the coil; we therefore used two interchangeable coils to obtain different polarizations of the alternating electric field. The axis of one was parallel to the long side of the plate, and that of the other to the short side (Fig. 2). The oscillation frequency varied from experiment to experiment in the interval from 2 to 10 Mcs. The coils were glued on a polystyrene plate and encased in a copper vacuum-type vessel which was inserted into the Dewar. The heat exchange gas was contained in the copper vessel.

The field produced by the electromagnet was horizontal and could be varied from zero to 10 kOe. The cryostat could be rotated about the vertical axis through any angle and also inclined ±4° to the magnetic field. The rotating unit was secured directly on the electromagnet, so that the latter served simultaneously as a massive base to reduce the vibrations of the cryostat. The circuit was sensitive enough to detect a nuclear-magnetic-resonance signal produced by protons in the polystyrene plate and by copper nuclei in the wire of the inductance coil. This produced field markers directly on the curves and made it possible to monitor the stability of the Hall pickup, whose voltage was fed to a two-coordinate automatic plotter.

4. EXPERIMENTAL RESULTS

We investigated the region of magnetic-field directions in the vicinity of the crystallographic axis [100]. For convenience in systematization and discussion of the results, this vicinity is shown in Fig. 3. The smallness of the angle intervals made it possible to use a rectangular projection. The dashed lines show the planes in which the direction of the magnetic field was varied in definite series of experiments.

Starting with approximately 2 kOe, the plot of $\partial f/\partial H$ vs. H assumes a sharply nonmonotonic and oscillating character (see Figs. 5—7). In weaker fields, the oscillations disappear and the monotonic component of $\partial f/\partial H$ increases. Simultaneously, a change takes place in the phase of the frequency modulation compared with the phase of the field modulation. This shows, apparently, that in weak fields, when the transverse conductivity of the metal is still large, the modulating field does not fully penetrate into the sample. It is possible that this is precisely why we were unable to observe the size effect in weak fields.

We established that the oscillations observed in fields of 2—10 kOe are periodic in a straight field and that the magnitude of the period ΔH does not depend on the temperature or frequency and is inversely proportional to the thickness of the sample. We have observed several groups of oscillations. Their interference sometimes makes it difficult to interpret the curves (for example, the lower curve on Fig. 6 below). However, in the immediate vicinity of the [100] direction the picture becomes simpler. This has made it possible to investigate in detail the angular dependences of the two groups of oscillations, which we shall arbitrarily call α- and β-oscillations.
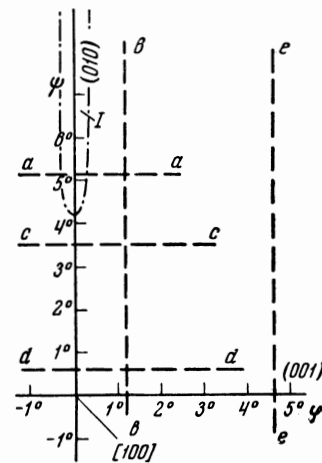

FIG. 3. Rectangular projection of the vicinity of the [100] axis on the direction sphere.
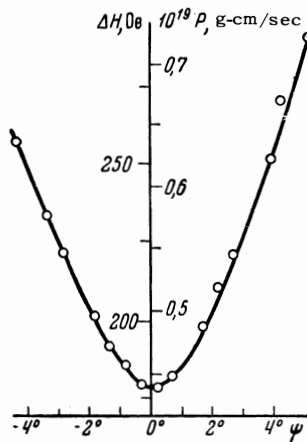
FIG. 4. Variation of the period of the α-oscillations when the magnetic field is rotated along the line bb. The numerical values of ΔH pertain to sample 2.

A. α-Oscillations. These are seen only for an ac electric-field polarization $\mathbf{E} \parallel [010]$. Figure 4 shows the dependence of the period of oscillations on the angle when the field direction varies along the line bb (Fig. 3). The value of P, represented by the second ordinate scale of Fig. 4, is obtained by multiplying ΔH by $de/2\pi c$, and has the meaning of a characteristic momentum. If the oscillations are determined by the electrons near the limiting point, then $P = K^{-1/2}$, and in the case of spiral trajectories $P = (2\pi)^{-1}(\partial S/\partial p_H)_{ext}$. When the vector $\mathbf{H}$ is rotated in another plane (for example along cc or dd) 5° from the (010) plane, the period increases only 2.5%. The oscillations are almost sinusoidal everywhere except the narrow region of angles near the (010) plane (region I of Fig. 3). As can be seen from the plots on Fig. 5, when $\mathbf{H}$ lies in this angle region the period of the α-oscillations doubles. The change in the period is nonmonotonic: the conserved extrema remain practically in their previous positions. Nothing of this kind is observed for oscillations with other periods in region I.

B. β-Oscillations. These are approximately one order of magnitude less intense than the α-oscillations. The shown plots of the β-oscillations pertain to a polarization $\mathbf{E} \parallel [001]$. However, in the field interval 1—2.5 kOe, β-oscillations are seen also for a polarization $\mathbf{E} \parallel [010]$, but then drop out against the background of the stronger α-oscillations. Thus, apparently, the amplitude of the oscillations depends less on the polarization. The series of plots shown in Fig. 6 corresponds to rotation of the vector $\mathbf{H}$ along the line bb. As in the case of the α-oscillations, the periods are practically independent of the angle φ. When $\varphi \gtrsim 4°$ (line ee), other periods also appear, so

that it becomes practically impossible to separate the β oscillations. The picture becomes more complicated also when the angle ψ increases (lower curve of Fig. 6).

C. γ-Oscillations. At angles $\varphi \sim 15-20°$ ($\psi \sim 0°$) we see again a distinct single period (Fig. 7) with p = 0.27 × 10^{-19} g-cm/sec. The γ-oscillations are seen equally well at both polarizations.

D. Long-Period oscillations. On sample 2, at $\mathbf{E} \parallel [010]$ and at small values of the angles φ and ψ, we could see quite clearly, besides the α-oscillations, long-period oscillations corresponding to p = 2.2 × 10^{-19} g-cm/sec —the same value as obtained in [4] for the limiting point I. However, these oscillations could not be seen with thinner samples, and also with a different polarization in sample 2.

5. DISCUSSION

The periodicity in the straight field and the harmonic character of the oscillations at the employed experimental geometry give grounds for assuming that the observed oscillations are due to the size effect produced by ineffective electrons. It is quite difficult to distinguish between the electrons at the limiting points and the electrons on helical trajectories, because the only practical criterion is the character of the dependence of the amplitude of the oscillations on the field. By employing this criterion it is possible, for example, to conclude that the β-oscillations are connected with the limiting points and the γ-oscillations with the helical tra-
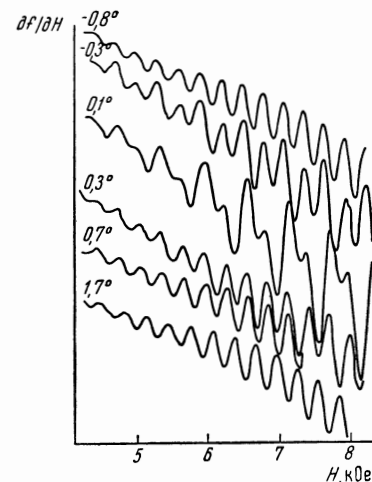

FIG. 5. Plots of the α-oscillations of sample 2 when the field is rotated along the line aa; $\mathbf{E} \parallel [010]$, T = 1.3°K, f = 5.0 Mcs. The curves are labeled with approximate values of the angle φ. (The angles were measured with approximate accuracy 10′, and the position $\varphi = 0°$ was determined from the symmetry of the effect.)

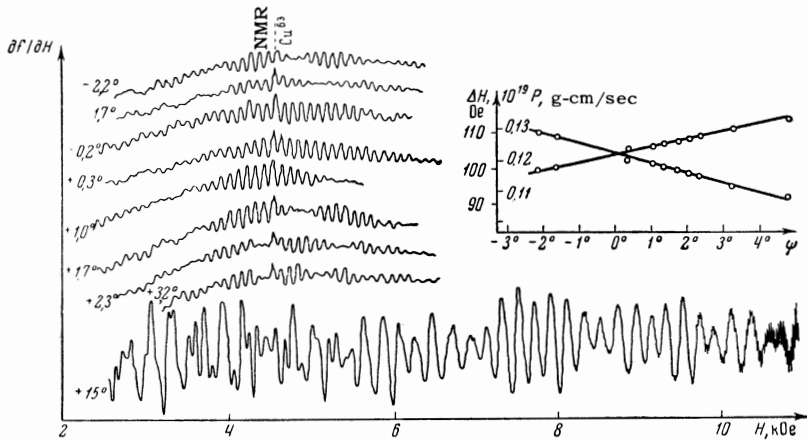FIG. 6. Plots of the oscillations in sample 1, with the field rotated along the line bb and with polarization E|| [001]; T = 1.3°K, f = 5.1 Mcs. The curves are marked with the values of the angle ψ. In the right side of the lower curve are seen the quantum oscillations of the impedance[15]. The relative nuclear magnetic resonance amplitudes and the amplitudes of the quantum oscillations are reduced by several times compared with the amplitude of the oscillations of the size effect, owing to a large rate of change of the field during the time of recording.

jectories. However, it is difficult to analyze the field dependence of the amplitude in our experiments because a slight penetration of the modulating field into the sample is possible in the case of weak fields, while in fields near 8—10 kOe the condition $u \gg \delta$ no longer holds. Therefore deductions based on an analysis of the amplitude of the oscillations are not very reliable.

On the other hand, we were unable to observe reliably oscillations from limiting points, which, according to our earlier data[4], should certainly exist in the vicinity of the [100] direction. The reason is not quite clear, all the more since the radius of curvature of the Fermi surface in the vicinity of the limiting point I is larger, and consequently the amplitude of the corresponding oscillations should also be large [see (13)]. It is possible that the oscillations due to the limiting points are generally indistinguishable against the background of oscillations from the helical trajectories the amplitudes of which are larger by a factor $(d/u)^{1/2}$.

We must dwell especially on the α-oscillations. They can be distinguished from the other groups by the very strong dependence of the amplitude on the polarization of the high-frequency field, and also by the already noted doubling of the period of the oscillations in a definite region of magnetic-field directions. The latter is probably due to the fact that at these field directions two identical closed orbits

merge into one, with a narrow neck in the middle. In such a case, the doubling of the period would be evidence of the presence of saddle points and orbits with self-intersection. At the same time, from other experiments with tin we know that the following takes place: In the same region of directions (i) a sharp increase in the amplitude and a narrowing of the lines, as observed by Koch and Kip[16] in cyclotron resonance in the normal field, and (ii) open trajectories appear on the Fermi surface of the fourth zone[13]. It is possible that some connection exists between these phenomena. For a final answer to the question of what groups of electrons cause the observed oscillations, we must know more details about the structure of the Fermi surface of tin.

The effect described above gives in principle the same information on the electron spectrum as the oscillations of the static conductivity of plates in a normal magnetic field[6-10]. The radio-frequency size effect appears preferable to us because, according to theory[6,7], the amplitude of the static-conductivity oscillations should decrease quite rapidly with increasing magnetic field. We note also that when a radio-frequency procedure is used, the measurements are carried out by contactless methods and samples with large area can be employed. However, it is still difficult to compare the possibilities of these two methods, owing to the lack of experimental material.
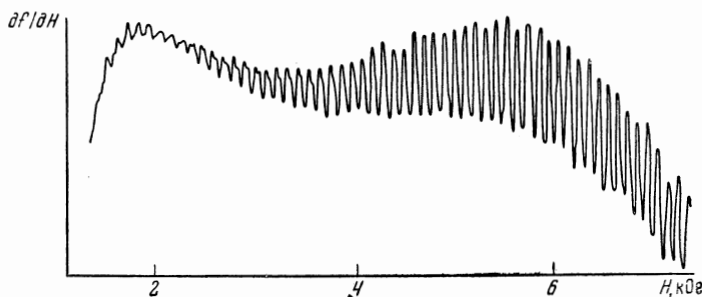

FIG. 7. Plot of the γ-oscillations in sample 2; E|| [010]. T = 1.3°K, f = 5.2 Mcs, $\varphi = 17°$, $\psi \approx 0°$.

[1] M. Ya. Azbel', JETP **39**, 400 (1960), Soviet Phys. JETP **12**, 283 (1961).

[2] V. F. Gantmakher, JETP **43**, 345 (1962), Soviet Phys. JETP **16**, 247 (1963).

[3] É. A. Kaner, JETP **44**, 1036 (1963), Soviet Phys. JETP **17**, 700 (1963).

[4] V. F. Gantmakher and É. A. Kaner, JETP **45**, 1430 (1963), Soviet Phys. JETP **18**, 988 (1964).

[5] V. F. Gantmakher and I. P. Krylov, JETP **47**, 2111 (1964), Soviet Phys. JETP **20**, 1418 (1965).

[6] E. H. Sondheimer, Phys. Rev. **80**, 400 (1950).

[7] V. L. Gurevich, JETP **35**, 668 (1958), Soviet Phys. JETP **8**, 464 (1959).

[8] J. Babiskin and P. G. Siebenmann, Phys. Rev. **107**, 1249 (1957).

[9] Zebouni, Hamburg, and Mackey, Phys. Rev. Letters **11**, 260 (1963).

[10] J. A. Munarin and J. A. Marcus, Paper at Ninth International Conference on Low Temperature Physics, USA, 1964.

[11] G. E. H. Reuter and E. H. Sondheimer, Proc. Roy. Soc. **195**, 336 (1949).

[12] M. Ya. Azbel' and M. I. Kaganov, DAN SSSR **95**, 41 (1954).

[13] V. F. Gantmakher, JETP **44**, 811 (1963), Soviet Phys. JETP **17**, 549 (1963).

[14] Yu. V. Sharvin and V. F. Gantmakher, PTÉ No. 6, 165 (1963).

[15] E. P. Vol'skiĭ, JETP **46**, 123 (1964), Soviet Phys. JETP **19**, 89 (1964).

[16] J. F. Koch and A. F. Kip, Phys. Rev. Letters **8**, 473 (1962).